technical note technical note

Energy Release by Rechargeable Lithium-Ion Batteries in Thermal Runaway

Richard E. Lyon and Richard N. Walters

April 2016

DOT/FAA/TC-TN16/22

U.S. Department of Transportation
Federal Aviation Administration

NOTICE

Technical Report Documentation Page

1. Report No.	2. Government Accession No.	3. Recipient's Catalog No.
DOT/FAA/TC-TN16/22		

4. Title and Subtitle	5. Report Date
ENERGY RELEASE BY RECHARGEABLE LITHIUM-ION BATTERIES IN THERMAL RUNAWAY	April 2016
	6. Performing Organization Code

7. Author(s)	8. Performing Organization Report No.
Richard E. Lyon and Richard N. Walters	

9. Performing Organization Name and Address	10. Work Unit No. (TRAIS)
Federal Aviation Administration William J. Hughes Technical Center Fire Safety Branch Aviation Research Division Atlantic City International Airport, NJ 08405	11. Contract or Grant No.

12. Sponsoring Agency Name and Address	13. Type of Report and Period Covered
U.S. Department of Transportation Federal Aviation Administration Northwest Mountain Region- Transport Airplane Directorate 1601 Lind Avenue, SW Renton, WA 98057	Technical Note
	14. Sponsoring Agency Code ANM-115

15. Supplementary Notes

16. Abstract

The energy released by failure of rechargeable 18-mm diameter by 65-mm long cylindrical (18650) lithium-ion cells/batteries was measured in a bomb calorimeter for four different commercial cathode chemistries over the full range of charge using a method developed for this purpose. Thermal runaway was induced by electrical resistance (Joule) heating of the cell in the nitrogen-filled pressure vessel (bomb) to preclude combustion. The total energy released by cell failure, ΔH_f, was assumed to be comprised of the stored electrical energy E (cell potential x charge) and the energies of mixing, chemical reaction, and thermal decomposition of the cell components, ΔU_{rxn}. The contribution of E and ΔU_{rxn} to ΔH_f was determined, and the mass of volatile, combustible thermal decomposition products was measured in an effort to characterize the fire safety hazard of rechargeable lithium-ion cells.

17. Key Words	18. Distribution Statement
Energy, Heat, Lithium-ion battery, Calorimetry, Thermal runaway, Fire hazard	This document is available to the U.S. public through the National Technical Information Service (NTIS), Springfield, Virginia 22161. This document is also available from the Federal Aviation Administration William J. Hughes Technical Center at actlibrary.tc.faa.gov.

19. Security Classif. (of this report)	20. Security Classif. (of this page)	21. No. of Pages	22. Price
Unclassified	Unclassified	26	

ACKNOWLEDGEMENTS

The authors are indebted to Professor James Quintiere (University of Maryland, College Park) for helpful discussions. Certain commercial equipment, instruments, materials, and companies are identified in this paper to adequately specify the experimental procedure. This in no way implies endorsement or recommendation by the FAA.

TABLE OF CONTENTS

LIST OF FIGURES

LIST OF TABLES

LIST OF ACRONYMS

LIB	Lithium-ion battery
SOC	State of charge

EXECUTIVE SUMMARY

The thermal energy released by failure of rechargeable 18-mm diameter x 65-mm long (18650) cylindrical lithium-ion cells (ΔH_f) was measured using a bomb calorimeter and a method developed for this purpose. It was found that the total energy released at failure ΔH_f is comprised of stored electrical energy, E, and chemical reaction energy, ΔU_{rxn}, in approximately equal parts for 3 of the 4 cell chemistries tested. Self heating of the cell during thermal runaway and burning or explosion of the volatiles ejected at failure have been identified as the primary fire hazards through full-scale testing, and both of these are found to be proportional to the total released at failure, ΔH_f. Because ΔH_f is proportional to the stored electrical energy E (cell potential x charge), the best single measure of the fire hazard of rechargeable lithium ion cells/batteries would be the maximum capacity of the cell E_{max} times the fractional (state of) charge Z, since $\Delta H_f \propto E = ZE_{max}$.

BACKGROUND

Rechargeable lithium-ion batteries (LIBs) are being used at an increasing rate because of their high energy density and their ability to be used repeatedly with little degradation in performance [1, 2]. Research to produce higher capacity lithium-ion batteries [3, 4] with better safety systems [5] is ongoing. Greater capacity means more stored energy to do electrical work, but can also mean greater thermal hazard if this energy is released suddenly because a contaminant, manufacturing defect, mechanical insult, overcharging, or the heat of a fire [6, 7] causes an internal short circuit. An internal short circuit results in a rapid discharge of electrical energy inside the cell that raises its temperature and causes mixing, chemical reactions, and thermal decomposition of the cell components in an auto-acceleratory, exothermic process called thermal runaway, which generates combustible gases and results in expulsion of the cell components [6–9]. Thermal runaway is propagated by the heating of adjacent cells in closely spaced bulk shipments; the combustible volatiles released at failure can accumulate in the compartment and cause a conflagration or explosion if ignited [6–9].

In a previous laboratory study at the FAA, the energy released by cylindrical 18-mm diameter by 65-mm long (18650) lithium-ion cells/batteries during thermal runaway was measured using a purpose-built thermal capacitance calorimeter [9]. These thermal energy release measurements were based on the temperature history of the LIB in an open system. The total energy released during thermal runaway could not be measured because the cell contents were ejected into the room at failure and the energy released by mixing, reaction, and thermal decomposition of the cell components occurred largely outside of the cell/calorimeter. The combustion energy released when the contents of lithium metal (non-chargeable) and lithium-ion (rechargeable) cells discharged at failure and burned in air was measured separately in a fire calorimeter and was found to be comparable in magnitude to the thermal energy released by cell failure [9].

This study is an attempt to measure the energies of the component processes of thermal runaway of 18650 LIBs by measuring the total energy at failure as a function of the stored electrical energy. This study's approach is to use electrical resistance (Joule) heating to drive the cell into thermal runaway inside the closed pressure vessel of a bomb calorimeter filled with one atmosphere of pure nitrogen. In this way, the cell contents are confined to the pressure vessel (bomb), and the heat and volatiles released at failure are generated in an inert environment that precludes burning or oxidation of combustibles.

THERMODYNAMICS OF BATTERY FAILURE IN A BOMB CALORIMETER

Rechargeable lithium-ion cells exchange lithium ions through electrolytes between positive and negative electrodes separated by ion-permeable polymer membranes. The electrolytes are typically lithium salts dissolved in high-purity linear and cyclic organic carbonates that are combustible [1–7]. During normal use, electrons flow through the terminals and lithium ions flow through the electrolyte from the anode to the cathode in a quasi-reversible process with negligible change in the chemical structures of the cell components. When a lithium-ion cell fails because of an internal short circuit, the resistance of the cell approaches zero and the current flows irreversibly between the electrodes, generating internal power of magnitude ε^2/Ω, where ε and Ω are the cell potential (V) and internal resistance (Ohms) of the cell, respectively. The power generated by an internal short circuit quickly exceeds the external heat losses, so the cell

temperature increases until the polymer separator melts and the electrodes and electrolytes mix, react, and thermally decompose.

When this process of cell failure happens in an adiabatic bomb calorimeter at constant volume [10], the temperature of the calorimeter increases from T_1 to T_2, but no work is done and no heat is transferred to the environment. Applying the first law of thermodynamics to the calorimeter system, the change in internal energy is zero for failure of the lithium-ion cell (i.e., U_2-U_1 = 0). However, if the masses and heat capacities of the reactants (virgin cell) and products (failed cell) are not significantly different, the internal energy change of the cell at failure in the pressure vessel ΔU can be obtained from a fictive process in which the heat required to raise the calorimeter temperature from T_1 to T_2 is estimated from the heat capacity, C, of the system (cell + calorimeter) [10]:

$$\Delta U = -C(T_2 - T_1) = \Delta U_{ext} + \Delta U_{elec} + \Delta U_{rxn} \tag{1}$$

In this study, it is assumed that the internal energy change measured in the bomb calorimeter test is the result of three processes represented by the right side of equation 1. These are the external electrical resistance (Joule) heating of the cell to failure (ΔU_{ext}), the discharge of stored electrical energy via an internal short circuit when the separator melts (ΔU_{elec}), and the exothermic, auto-acceleratory chemical and physical changes of the cell contents during the ensuing temperature rise (ΔU_{rxn}). The Joule heat used to force the lithium-ion cells into thermal runaway in the bomb calorimeter is:

$$\Delta U_{ext} = U_{ext} = -\int_0^{\tau} VI\,dt = -VI\tau \tag{2}$$

In equation 2, V and I are the measured voltage and current in a resistance heating wire connected to an external power source at time, t, and τ is the duration of Joule heating. The stored electrical energy released by an internal short circuit when the separator fails is:

$$\Delta U_{elec} = -\int_0^{\infty} \frac{\varepsilon^2}{\Omega} dt = -\int_0^{\infty} \varepsilon i\,dt \approx -\varepsilon \int_0^{t_c} I dt = -\varepsilon Q = -E \tag{3}$$

In equation 3, i is the internal current associated with a short circuit and Q is the charge on the cell in Coulombs (A-s) after being connected to an external current source (charging device) for duration, t_c. The release of electrical energy, E, when the polymer separator melts results in a rapid increase in the cell temperature, causing the cell components to mix, chemically react, and thermally decompose to liquid, solid, and gaseous products in an irreversible process:

$$\text{Electrolytes + Electrodes + Separator} \rightarrow \text{Liquid, Solid, and Gaseous Products} \tag{4}$$

The internal energy change for the mixing, chemical reactions, and thermal decomposition of the cell components is ΔU_{rxn} in equation 1. From equations 1–4, the internal energy change of an adiabatic calorimeter system associated with lithium-ion cell failure is:

$$\Delta U = -C\,\Delta T = -E + \Delta U_{rxn} - VI\tau \tag{5}$$

Therefore, the internal energy change of the lithium-ion cell at failure is:

$$\Delta U_f = -E + \Delta U_{rxn} = -C\,\Delta T + VI\tau \tag{6}$$

The energy released when a lithium-ion cell fails at constant (atmospheric) pressure, *P*, is the enthalpy, which is related to the quantities measured in the bomb calorimeter at constant volume:

$$\Delta H_f = \Delta U_f + \frac{m_g R T_1}{M_g} \tag{7}$$

Ideal gas behavior is assumed for equation 7, with m_g and M_g being the mass and average molecular weight of the volatiles produced at failure, respectively, and *R* being the gas constant. Empirically, it is found that ΔU_f and ΔH_f are negative with respect to the system because the change in these state functions at cell failure is accompanied by an increase in the temperature of the system (calorimeter) so that heat seeks to flow to the surroundings. From the authors' perspective in the surroundings, these quantities have positive values and this convention will be used throughout this report for convenience after properly accounting for the signs in equation 7.

MATERIALS

The batteries used in this study consisted of lithium transition-metal oxide cathodes ($LiCoO_2$, $LiNiCoO_2$, $LiNiCoAlO_2$, $LiMn_2O_4$, etc.) in contact with an aluminum terminal and a graphitic carbon anode attached to a copper terminal. A liquid electrolyte comprised of lithium salt and organic solvents is contained between the electrodes [1–7]. In the rechargeable LIBs of this study, the cell is made in sheet form and rolled to fit inside a cylindrical steel jacket measuring 18 mm in diameter and 65 mm in length. These cells were purchased from commercial sources. Assemblies of these lithium-ion electrochemical cells designed for a specific purpose are called batteries. Table 1 lists the cathode chemistry; rated and measured charged capacity in Coulombs, Q_{max}(A-s); the nominal and measured cell potential, ε(V); and the mass, m_0, of the 18650 lithium-ion cell/battery. Also listed are the maximum electrical capacity of the cell, $E_{max} = \varepsilon_{max} Q_{max}$, and the specific electrical energy of the cell, E_{max}/m_0. The nitrogen gas used to inert the bomb calorimeter was an ultra-high-purity (>99.99%) grade obtained from a local supplier.

Table 1. Room temperature properties of rechargeable lithium-ion 18650 batteries at maximum electrical capacity

Cathode Chemistry	Charge Capacity, Q_{max} (A-s)		Cell Potential, ε(V)		Cell Mass, m_0 (kg)	E_{max} (kJ/cell)	E_{max}/m_0 (Wh/kg)
	Rated	Measured	Nom.	Max.			
$LiMn_2O_4$-$LiNiCoO_2$	11,700	11,500	3.6	4.1	0.042	47	312
$LiCoO_2$	9,400	8,700	3.7	4.1	0.048	36	206
$LiNiCoAlO_2$	5,400	5,200	3.7	4.1	0.042	21	141
Unknown	18,000	4,000	3.7	4.0	0.040	16	111

METHODS

BATTERY CHARGING

The electrochemical cells in table 1 were charged to various Q using a commercial charging device (Model X4AC, HiTec RCD, Poway, California) that could simultaneously charge four batteries while providing Q and ε for the individual cells [11]. The charge, Q, is the electrical capacity of the cell in Coulombs (A-s), which is related to the more conventional measure of charge, 1 mAh = 3.6 A-s. Zero charge (Q = 0) was obtained by completely draining the cell by first discharging to the minimum 2.9 volts for these LIBs with the charger, then using a small light bulb connected to the terminals to drain the cell to zero volts (as indicated by the charger and the absence of luminosity). By this procedure, the fractional charge recorded and reported for the cells of this study is the absolute fraction of the measured charge capacity of the cell:

$$Z = \frac{Q}{Q_{max}} \tag{8}$$

The fractional capacity used in this study differs from the conventional definition of state of charge (SOC), which is a relative value based on the operating range and rated charge capacity of the cell. Typically, 15%–20% of the rated capacity is left in the cell at zero SOC to prolong the life of the cell. Figure 1 is a plot of cell potential, ε, versus fractional charge, $Z = Q/Q_{max}$, for typical rechargeable lithium-ion 18650 cells/batteries at different ambient temperatures. Note that ε versus Z plots converge to a single curve with increasing temperature.

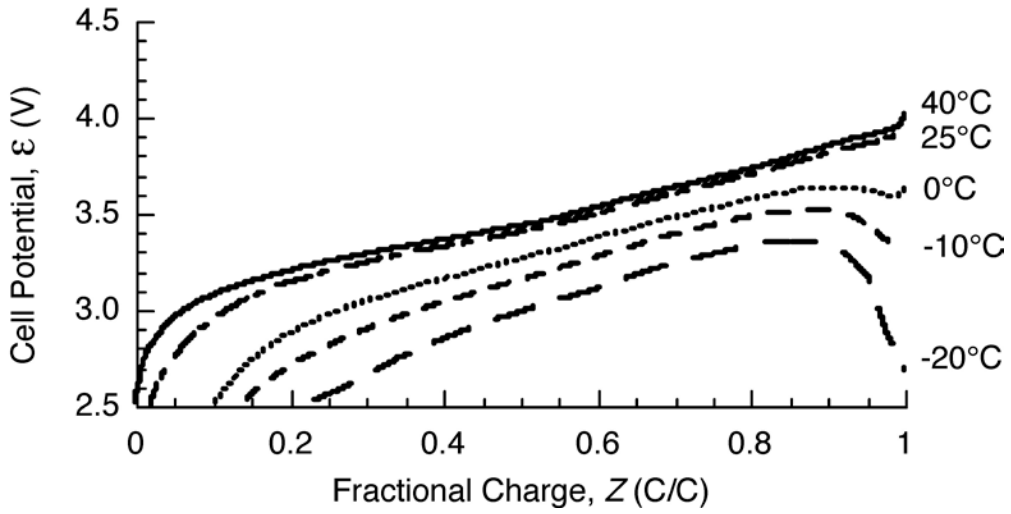

Figure 1. Cell potential (ε) vs. fractional charge (*Z*) at indicated temperatures for a typical 18650 LIB

BOMB CALORIMETER MEASUREMENTS

The violent ejection of cell components at cell failure and the generation of gaseous, combustible thermal decomposition products at high temperature during thermal runaway [6–9] suggest that the energy of this process should be measured in a sealed pressure vessel under inert conditions. In this study, a static jacket bomb calorimeter (Model 1341, Plain Jacket Oxygen Bomb Calorimeter, Parr Instrument Company, Moline, Illinois) was modified for this purpose to allow electrical resistance (Joule) heating of a lithium-ion cell to failure inside a closed, constant-volume pressure vessel (bomb) [12]. Figure 2 is a schematic diagram of the pressure vessel of the bomb calorimeter modified for these experiments [11] using the same sample heating configuration that was used in the thermal capacitance calorimeter [9].

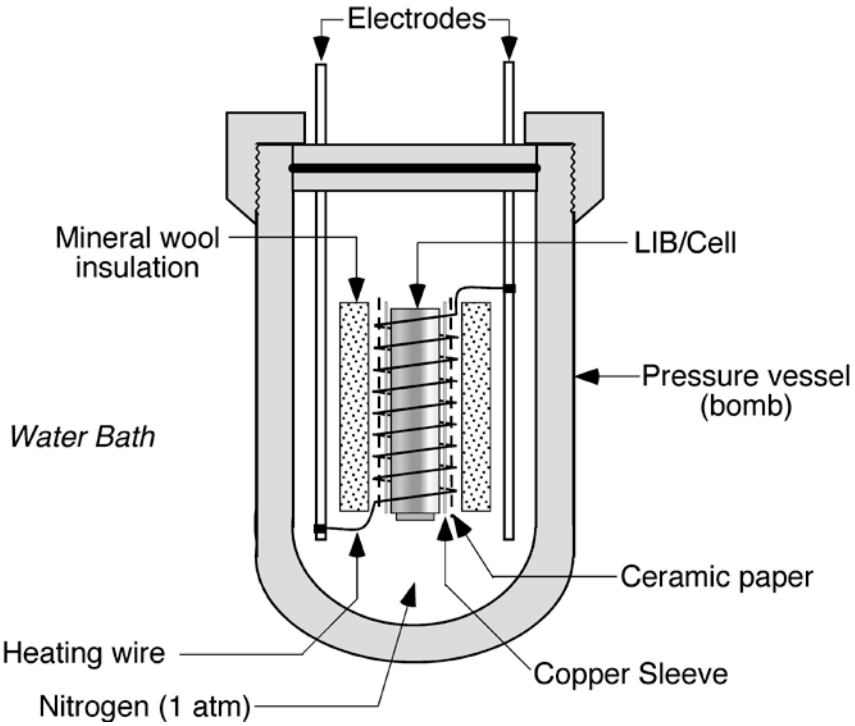

Figure 2. Pressure vessel of a static jacket bomb calorimeter modified to heat the 18650 LIBs to failure and measure the energy released

In the standard bomb calorimeter, the electrodes hold the sample cup and connect to the ignition wire. In the present modification [11], longer electrodes were used that served as leads to the electrical resistance wire used for Joule heating of the cell. Prior to testing, the plastic sheath was removed from the cell, and the cell was placed in a copper sleeve covered with a thin ceramic paper to electrically insulate the copper sleeve from a 46-cm length of 24-gauge nickel-chromium (Nichrome) resistance wire having a total resistance of 2.2–2.4 Ohms. The heating wire was wrapped around the cell/copper/paper assembly and connected to the terminal posts to make an electrical connection and suspend the cell in the bomb, as shown in Figure 2. The cell assembly was then wrapped in mineral wool (Kaowool®) insulation before placing it in the calorimeter pressure vessel (bomb) as per Quintiere et al. [9]. The bomb was purged several times with ultra-high purity nitrogen to remove all oxygen and sealed at 1 atmosphere of nitrogen pressure. Purging the bomb with nitrogen precludes any heat generation associated with the reaction of the cell components with atmospheric oxygen during the test. A voltage was applied to the resistance wire for 15 minutes to heat the cell to failure, which occurred approximately 10 minutes into the program at a temperature of approximately 200°C–250°C. The measured current (3A) and voltage (8V) for the 15-minute heating period were used to calculate the Joule heat, $U_{ext} = -VI\Delta t \approx -22$ kJ, that was added to the calorimeter for each experiment.

Standard methods of measuring heats of reaction in bomb calorimeters [12] are based on the thermal response of the calorimeter to an instantaneous heat pulse (e.g., combustion of a benzoic acid calibration standard). In the present method, Joule heat is generated at a constant rate over a relatively long period of time (15 minutes), and the sudden release of energy at cell failure is

superimposed on this heating history. Though thermal runaway occurs in a matter of seconds [9], the chemical reactions of the cell components may continue for an extended period of time in the inert pressure vessel. Moreover, the static jacket bomb calorimeter used for these experiments is only quasi-adiabatic, so a new method was developed to compute the total energy release of an arbitrary process in a static jacket calorimeter from the measured temperature history [13]:

$$\Delta U(t) = C_2\left(1+\frac{\tau_1}{\tau_2}\right)\Delta T(t) + K_2\int_0^t \Delta T(x)dx + C_2\tau_1\frac{d\Delta T(t)}{dt} - K_2\,(T_\infty - T_0) \qquad (9)$$

In equation 9, $\Delta T(t) = T(t)\text{-}T_0$ is the temperature rise of the water bath at time, t, from an initial temperature, T_0, when electrical resistance heating is initiated at $t = 0$ and T_∞ is the average ambient (room) temperature over the test duration. The coefficients C_2 and K_2 are the heat capacity and heat transfer coefficient of the calorimeter, respectively; τ_1 is the time constant of the pressure vessel; and $\tau_2 = C_2/K_2$ is the time constant for the entire calorimeter. For an adiabatic calorimeter, $K_2 = 0$ and $\tau_2 = \infty$. For the quasi-adiabatic static jacket bomb calorimeter from this study, the constants C_2, K_2, and τ_1 were obtained parametrically from a fit of equation 10 to the temperature history for a heat pulse of magnitude, q_0, imposed at time $t = 0$:

$$\Delta T(t) = \left(T_\infty - T_0\right)\left(1-e^{-t/\tau_2}\right) + \frac{q_0}{C_2(1-\tau_1/\tau_2)}\left(e^{-t/\tau_2} - e^{-t/\tau_1}\right) \qquad (10)$$

The contents of the bomb for these calibrations were identical to the battery tests, except that a 44-g aluminum cylinder having the same thermal mass as a rechargeable 18650 battery was used as a surrogate.

GRAVIMETRIC MASS LOSS MEASUREMENTS

In addition to measuring the cell failure energy in the bomb calorimeter, a gravimetric analysis was performed to determine the mass of cell components that were converted to gases at room temperature (gasification). Because the bomb is a closed system and the mass of reactants and products are equal, the mass of the bomb remained constant for the entire test, indicating that no products escaped or water leaked into the pressure vessel. Once the bomb was loaded with the sample and heating apparatus, it was purged with nitrogen and weighed to determine the initial mass. After the test the bomb was removed from the water bath, cooled to room temperature, wiped with a towel, and blown dry with compressed air. The dry, final weight was measured to ensure that no leakage occurred, and the bomb was vented to release gaseous reaction and decomposition products into a fume hood or into a gas sample bag for further analysis by infrared spectroscopy. The bomb was then reweighed to obtain the mass of volatiles that escaped from the pressure vessel at room temperature after cell failure.

RESULTS AND DISCUSSION

CALIBRATION OF THE BOMB CALORIMETER

The thermal constants of the bomb calorimeter (C_2, K_2, and τ_1) were measured by fitting equation 10 to the temperature history for 10 combustion tests ranging in mass of benzoic acid from 0.966g–1.568g, for which the combustion heats ranged from q_0 = 25.62–41.54 kJ. In these calibration tests, q_0 is the heat released by complete combustion (reaction) of benzoic acid with oxygen (i.e., $\Delta U = \Delta U_{rxn} = q_0$). The calibration tests were conducted according to a standard method [12] in which the bomb is pressurized to 30 atmospheres with pure oxygen and the temperature rise of the water bath, ΔT, is measured as a function of time. Figure 3 shows the measured temperature history for a heat pulse of magnitude, q_0 = 25.6 kJ, resulting from benzoic acid combustion and the temperature history calculated using equation 10 with the average calorimeter constants from the 10 replicate benzoic acid calibration tests in table 2. The maximum temperature rise of the bomb calorimeter, ΔT_{max}, for the benzoic acid heat pulse is $\Delta T_{max} = q_0/C_2(1+\tau_1/\tau_2)$ [13], and this occurs at time $t_{max} = \tau_1\tau_2\ln[\tau_2/\tau_1]/(\tau_2-\tau_1) \approx 7$ minutes into the test, in agreement with the data in figure 3.

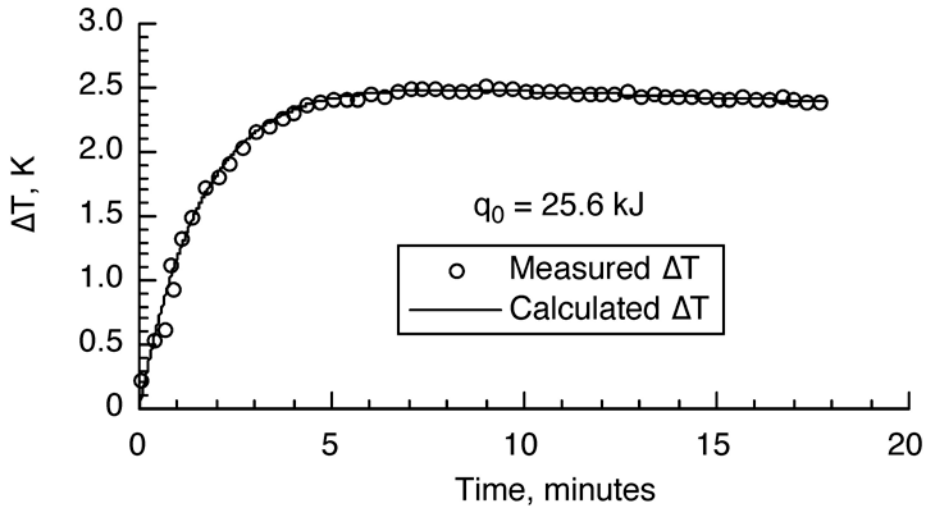

Figure 3. Measured and calculated temperature history of the modified bomb calorimeter for a benzoic acid heat pulse q_0 = 25,598 J using equation 10 and the thermal parameters in table 2

Table 2. Thermal parameters for modified bomb calorimeter of figure 2

C_2 (J/K)	τ_1 (min)	τ_2 (min)	$K_2 = C_2/\tau_2$ (W/K)
10,092 ± 216	1.21± 0.15	344 ±90	0.49 ±0.13W/K

Figure 4 is a plot of ΔT_{max} versus q_0 for the 10 benzoic acid combustion tests in the modified bomb calorimeter. The inverse slope of the best-fit line of figure 4 is called the energy equivalent of the calorimeter in standard methods [9]. A value, C = 10,262 J/K, is obtained for the modified bomb calorimeter of this study, which is within 1% of the theoretical value [13], $C = C_2(1+\tau_1/\tau_2)$ = (10,092 J/K)(1+1.2 min/344 min) = 10,127 J/K using the thermal parameters

in table 2. By comparison, the thermal parameters for the standard, unmodified, static jacket bomb calorimeter are: τ_1 = 1 minute; τ_2 = 550 minutes; C_2 = 9,952 J/K, and K_2 = 0.3 W/K [13].

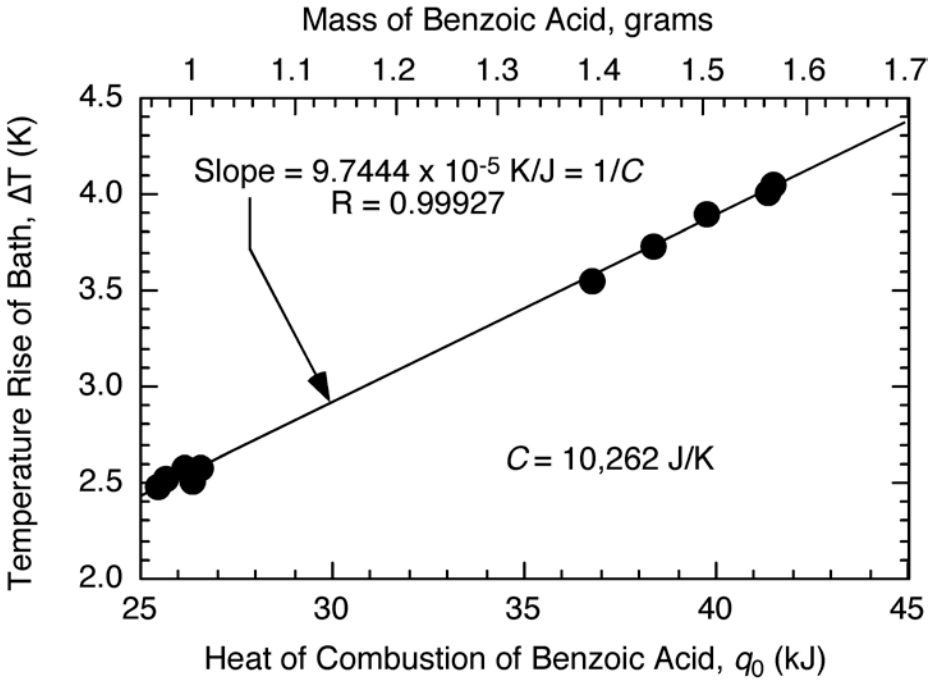

Figure 4. Benzoic acid calibration of modified bomb calorimeter

Figure 5A is a plot of equation 9 using the temperature history of figure 2 with the calorimeter thermal parameters in table 2. The noise in $\Delta U(t)$ at the beginning of the test is due to the temperature-time derivative, which is the second-to-last term in equation 9. Figure 5B is a locally weighted, nonlinear, least-squares curve-fit of $q(t)$ in figure 5A. The computed steady-state value in figure 5B is $\Delta U(\infty)$ = 25,590 ±140 J/g, which is indistinguishable from the heat of combustion of the benzoic acid, $\Delta U_{rxn} = q_0$ = 25,598 J. The excellent agreement between the known heat of a prescribed process, q_0, and the value $\Delta U(\infty)$ computed from the measured temperature history of the water bath validates equation 9 for measuring the energy released in the relatively long and complicated (arbitrary) process of electrical resistance heating of a lithium-ion cell to thermal runaway and failure.

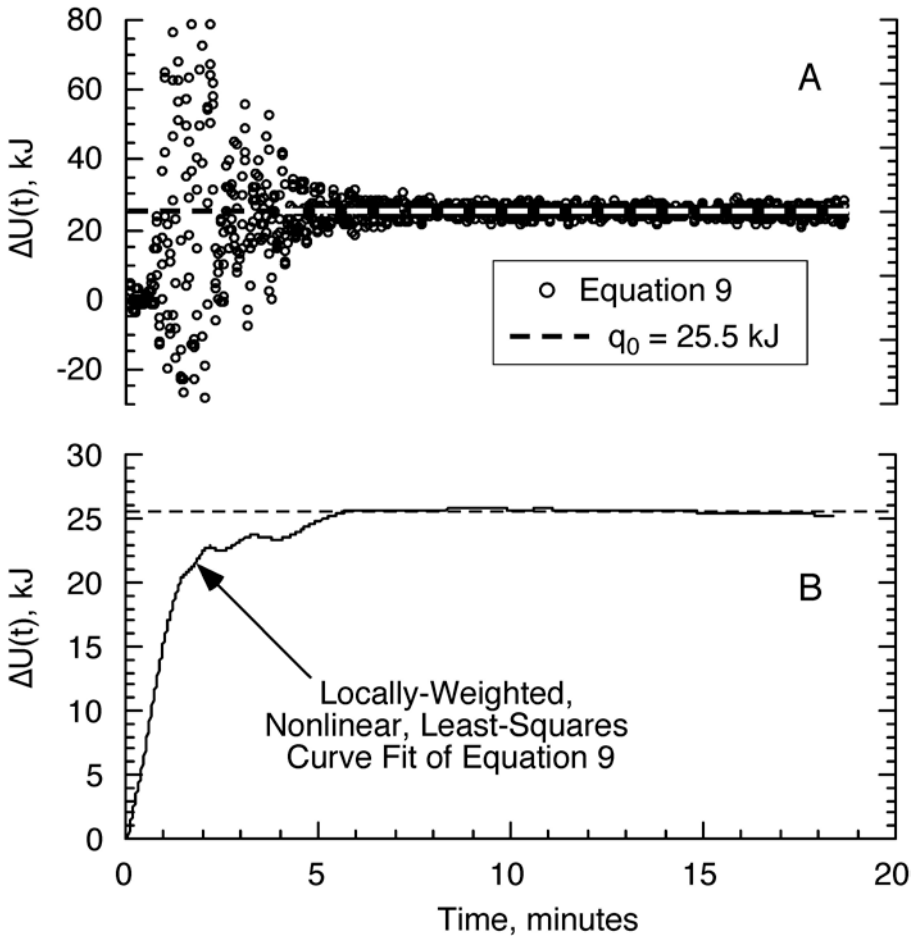

Figure 5. Plot of equation 9 for the temperature history in figure 3 with A) direct calculation with derivative noise and B) locally-weighted nonlinear least squares curve fit of direct calculation

ENERGETICS OF CELL FAILURE

Figure 6 is a composite plot of representative energy release histories, $\Delta U(t)$, calculated using equation 9 and the temperature histories of each LIB heated to failure in the bomb calorimeter at the indicated fractional charge, Z. The lithium-ion cells go into thermal runaway and rupture (fail) at approximately 10 minutes into the 15-minute Joule heating program, which is coincident with the steep rise in $\Delta U(t)$ in figure 5. These energy release histories include the electrical resistance (Joule) heat generated in the bomb over the Δt = 15 minute (900s) heating period. The Joule heat, U_{ext} = VIτ, for each experiment was subtracted from the plateau value of the heat release, $\Delta U(\infty)$, in figure 6 as per equation 6 to obtain ΔU_f for each cathode chemistry and fractional charge listed in table 3. The stored electrical energy, $E(Z)$, at each fractional charge, Z, was then subtracted from ΔU_f to obtain each heat of reaction, ΔU_{rxn}, in table 3 as per equation 6. Finally, the enthalpy of cell failure was calculated from the mass of gaseous products, m_g, using M_g = 28 g/mole as per equation 7. Each value in table 3 is an average of 3–5 replicate tests and the mean weighted coefficient of variation is approximately 7%.

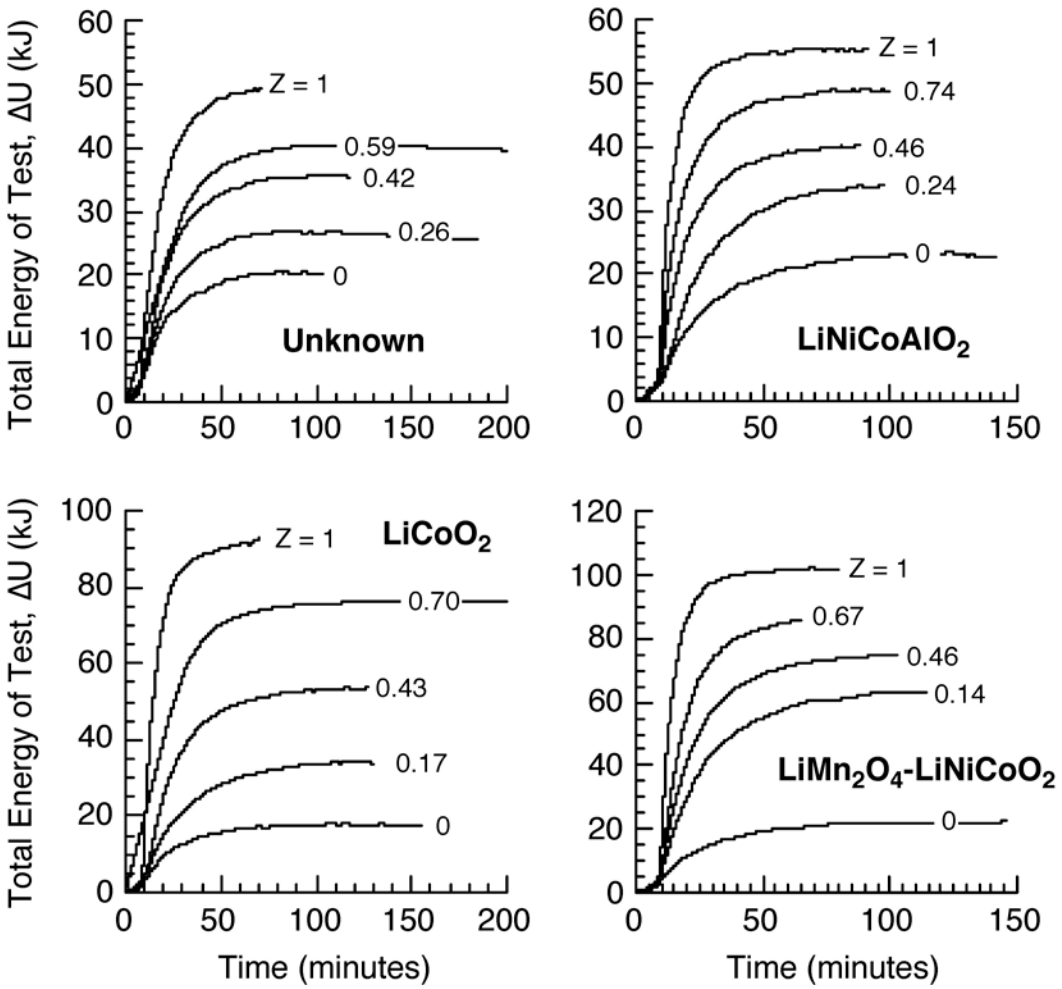

Figure 6. Total energy release histories, $\Delta U(t)$, for LIBs in bomb calorimeter at indicated fractional charge Z.

Table 3. Fractional charge (Z), charge (Q), cell potential (ε), stored electrical energy (E), failure energy (ΔU_f), reaction energy (ΔU_{rxn}), volatile mass (m_g), and failure enthalpy (ΔH_f) for 18650 LIBs

Cathode	Z (%)	Q (A-s)	ε (V)	E (kJ/cell)	ΔU_f (kJ/cell)	ΔU_{rxn} (kJ/cell)	m_g (g)	ΔH_f (kJ)
Unknown	0	0	0.00	0.00	-1.25	-1.25	0.46	-1.29
	26	1,062	3.57	3.79	8.92	5.13	1.03	8.83
	42	1,696	3.70	6.27	15.83	9.56	1.48	15.7
	59	2,372	3.64	8.64	19.61	10.97	1.73	19.46
	100	4,018	4.10	16.47	26.76	10.92	2.06	26.58
$LiNiCoAlO_2$	0	0	0.00	0.00	-1.50	-1.50	0.34	-1.53
	24	1,231	3.45	4.25	11.04	6.79	0.74	10.97
	46	2,398	3.58	8.58	19.04	10.46	1.58	18.90
	74	3,816	3.80	14.50	27.30	12.80	2.51	27.08
	100	5,173	4.10	21.21	37.53	16.32	2.95	37.27
$LiCoO_2$	0	0	0.00	0.00	-2.12	-2.12	0.29	-2.15
	17	1,519	3.42	5.20	15.38	10.18	0.50	15.34
	43	3,780	3.57	13.50	30.76	17.26	0.95	30.68
	70	6,109	3.70	22.60	50.62	28.02	2.20	50.43
	100	8,712	4.00	34.85	66.08	31.23	4.46	65.69
$LiMn_2O_4$-$LiNiCoO_2$	0	0	0.00	0.00	-0.08	-0.08	0.47	-0.12
	14	1,652	3.23	5.34	36.60	31.26	1.05	36.51
	46	5,227	3.44	17.98	50.87	32.89	2.63	50.64
	67	7,628	3.66	27.92	62.75	34.83	4.25	62.37
	100	11,455	4.10	46.97	78.14	31.17	5.47	77.66

Figure 7 is a composite plot of ΔH_f, E, and ΔU_{rxn} versus Z for all of the LIBs. It shows that chemical reaction energy, ΔU_{rxn}, and the electrical energy, E, contribute to ΔH_f at each fractional charge, Z. Note that $Z \approx 0.20$ is the lower limit of the operating range of LIBs, at which point ΔH_f is approximately 1/3 of the maximum for the cell. The chemical energy release of the common $LiCoO_2$ cell at maximum capacity in figure 7 and table 3, ΔU_{rxn} = 31 kJ, compares favorably to the sum of the separate anode decomposition and reaction with electrolyte (11 kJ), cathode decomposition and reaction with electrolyte (23 kJ), and self-reaction of salt with solvent (4 kJ) estimated for a 18650 $LiCoO_2$ lithium-ion cell of similar charge capacity [6].

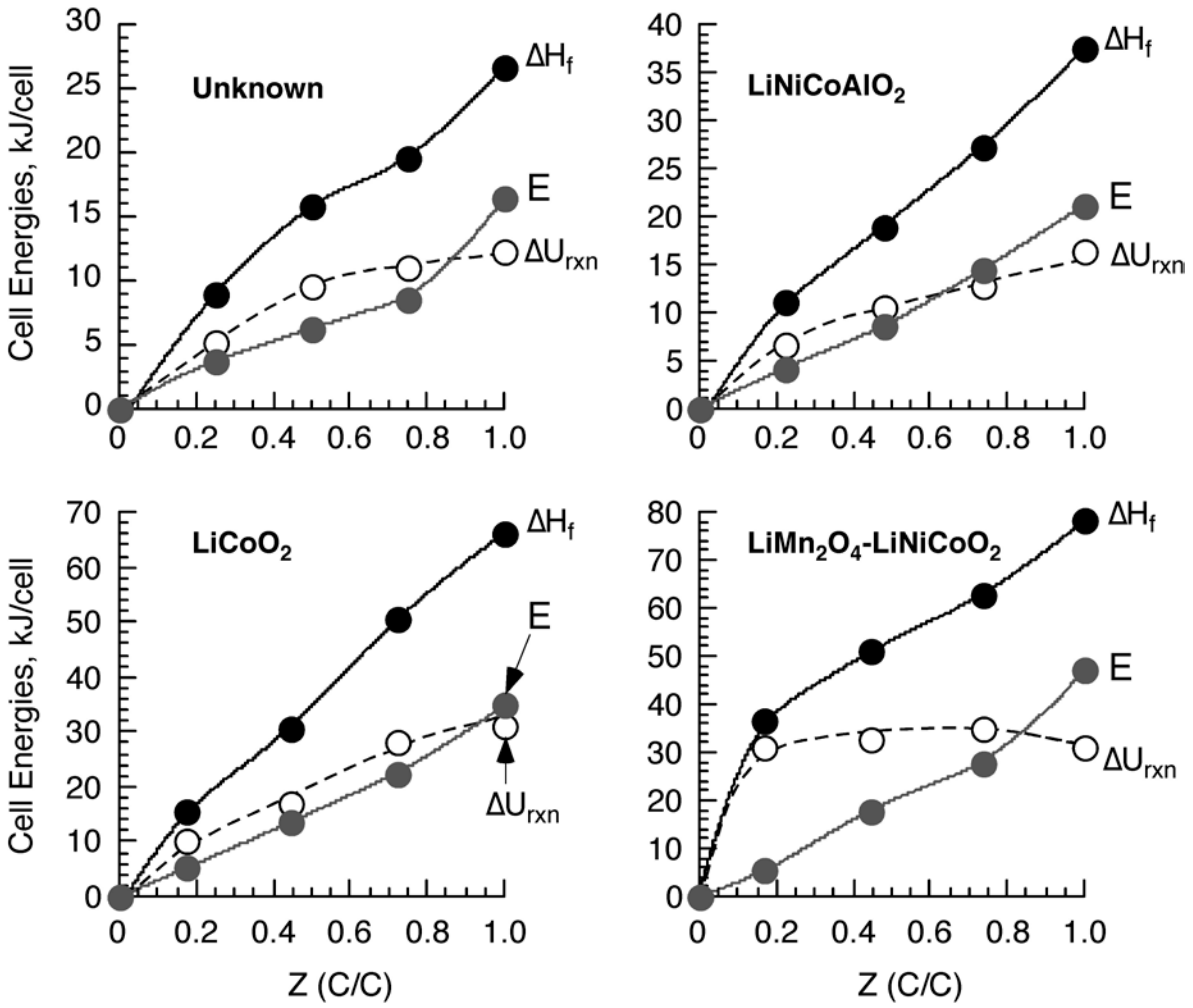

Figure 7. Failure enthalpy (ΔH_f), stored electrical energy (E), and chemical reaction energy (ΔU_{rxn}) released at cell failure vs. fractional charge (Z) for LIBs

Figure 8 is a plot of the total enthalpy release, ΔH_f, of the LIB in the bomb calorimeter versus: A) the stored electrical energy, E, and B) the fractional charge, Z. Clearly, E is a better predictor of total enthalpy of failure than Z for the lithium-ion cells of this study because, unlike Z, it is independent of the cathode chemistry and maximum cell capacity. The best-fit polynomial curve shown as the solid line in figure 8A for all of the cell chemistries ($R^2 = 0.91$), with E in kJ, is:

$$\Delta H_f\,(kJ) = 1.12 + 2.49E - 0.018E^2 \qquad (11)$$

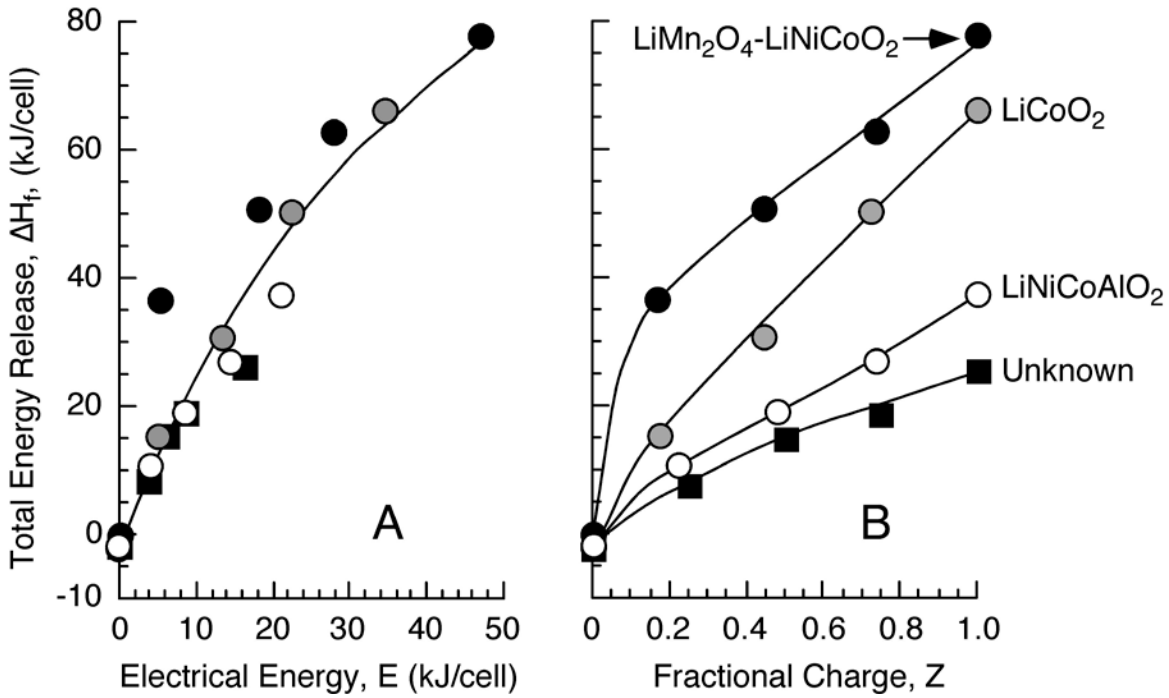

Figure 8. Total energy release, ΔH_f vs.: A) electrical energy, E, and B) fractional charge (Z) for the different LIB cathode chemistries

Figure 9 is a plot of the energy of the chemical reactions, ΔU_{rxn}, versus the stored electrical energy, E, for the LIBs. For most of the cells, ΔU_{rxn} is approximately proportional to E. However, the high-energy (see table 3) mixed metal oxide $LiMn_2O_4$-$LiNiCoO_2$ cathode cell is unique in that ΔU_{rxn} is essentially independent of E. One explanation for this observation is that the internal temperature of the cell during thermal runaway is sufficiently high at each fractional charge that the chemical reactions are forced to completion. The rate of internal energy generation during thermal runaway, which occurs in seconds, greatly exceeds the rate of heat removal from the cell surface by convection, conduction, and radiation. Consequently, the internal temperature, θ, of the cell during thermal runaway is essentially adiabatic and of the order:

$$\theta = \frac{\Delta H_f}{m_0 c_P} \tag{12}$$

For the $LiMn_2O_4$-$LiNiCoO_2$ cathode cells, m_0 = 0.042 kg (table 1), c_P = 1000 J/kg-K [9], and equation 12 shows that θ ranges from 800°C–1800°C for $Z > 0$ using the ΔH_f (see table 3). These temperatures are probably sufficient to force the chemical reactions of the mixed metal oxide cell components to completion during thermal runaway at all Z.

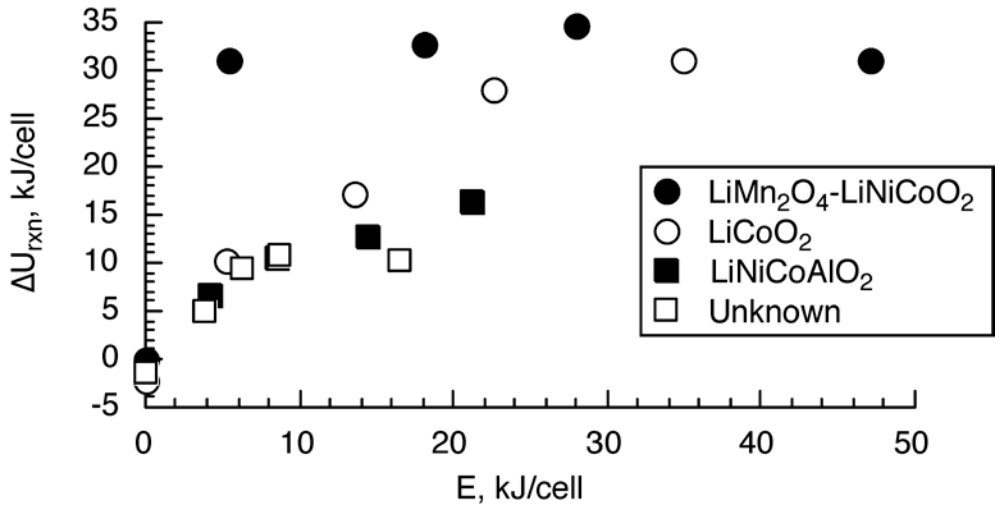

Figure 9. Energy of chemical reactions, ΔU_{rxn}, vs. stored electrical energy, E, for LIBs

Figure 10 is a plot of the maximum stored electrical energy, E_{max}, versus the average energy released by the chemical reactions of the LIB at cell failure, ΔU_{rxn}, over the useable range, Z = 0.2-1.0. From these limited data, it appears that the maximum electrical energy available from these cells is proportional to the chemical reaction energy of the cell components.

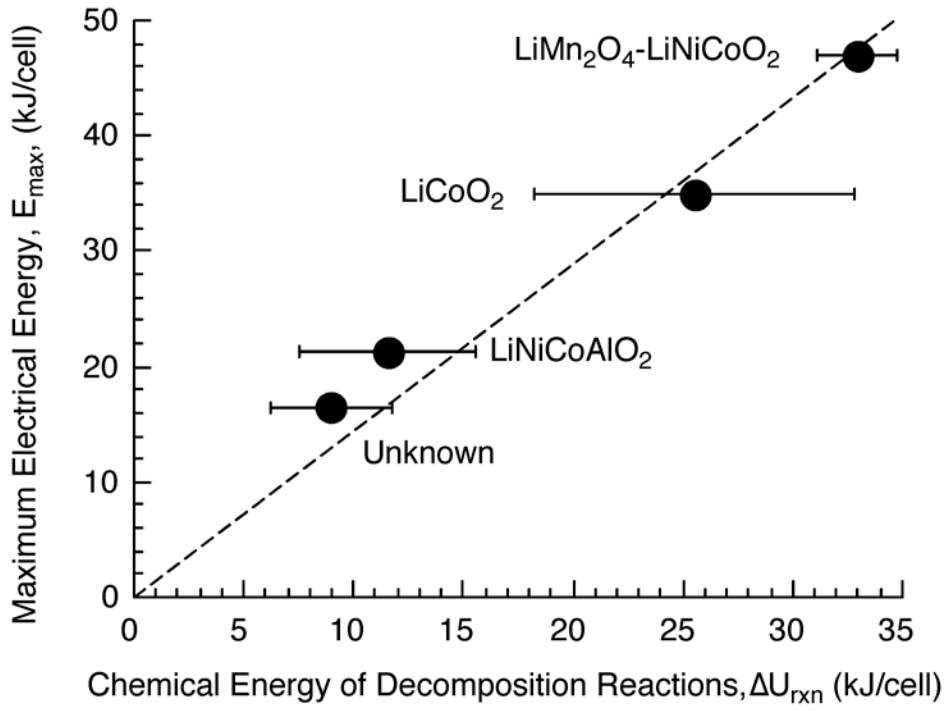

Figure 10. Maximum stored electrical energy, E_{max}, vs. energy of decomposition reactions, ΔU_{rxn}, for the different LIB cathode chemistries

GASIFICATION OF CELL CONTENTS AT FAILURE

Thermal decomposition of the cell components during thermal runaway generates products that are gases at room temperature [6–9]. The mass of cell contents converted to room-temperature volatiles was determined gravimetrically by weighing the bomb before the test and after venting to the atmosphere following the test. In some cases, volatiles continued to be produced by chemical reactions of the cell contents in the sealed, anaerobic bomb for several hours following the test. The total mass of gaseous products generated by thermal runaway for each cell versus E and Z is given in table 3 and plotted in figure 11. Figure 11A shows that the mass of volatiles produced at cell failure for all of the cathode chemistries is proportional to the stored electrical energy, E. In contrast, Figure 11B shows that volatile mass is highly dependent on cathode cell chemistry when fractional charge is the independent (predictor) variable.

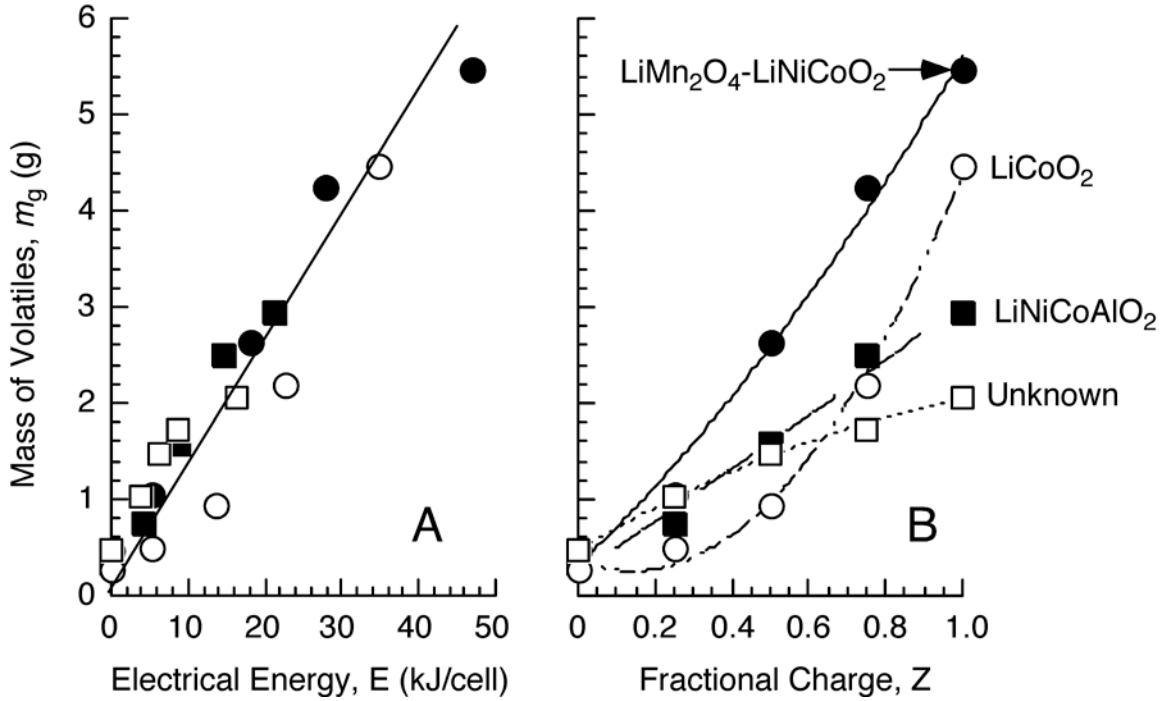

Figure 11. Mass of volatiles produced at cell failure vs.: A) electrical energy, *E*, and B) fractional charge, *Z*, for the LIBs

CONCLUSIONS

The energy/enthalpy released by thermal runaway and failure of rechargeable 18650 lithium-ion cells (ΔH_f) can be measured using a bomb calorimeter and a method developed for this purpose. It was assumed that ΔH_f is comprised of stored electrical energy, E, and chemical reaction energy, ΔU_{rxn}, and these were found to be approximately equal for 3 of the 4 cell chemistries tested. With regard to safety hazards, the large and rapid temperature rise of the LIB during thermal runaway θ, which drives failure propagation, is proportional to ΔH_f, which itself is proportional to E. Because the mass of combustible volatiles, m_g, is also proportional to E, a general measure of the fire hazard of LIBs for most of the cells tested in this study is the stored electrical energy, $E \approx ZE_{max}$.

REFERENCES

1. *Linden's Handbook of Batteries, 4th Edition*, Reddy, T.B. and Linden, D., eds., McGraw Hill, New York, 2011.

2. *Lithium Batteries: Science and Technology*, Nazri, G.A. and Pistoia, G., eds., Springer Publishers, New York, 2009.

3. Shukla, A.K. and Prem Kumar, T., "Materials for Next Generation Lithium Batteries," *Current Science*, Vol. 94, No. 3, 2008, pp. 314–331.

4. Li, J., Daniel, C., and Wood, D., "Materials Processing for Lithium-Ion Batteries," *Journal of Power Sources*, Vol. 196, 2011, 2452–2460.

5. Balakrishnan, P.G., Ramesh, R., and Prem Kumar, T., "Safety Mechanisms in Lithium-Ion Batteries," *Journal of Power Sources*, Vol. 155, 2006, pp. 401–414.

6. Barnett, B., Ofer, D., Sriramulu, S., and Stringfellow, R., "Lithium-Ion Batteries, Safety," in *Batteries for Sustainability*, Brodd, R.J., ed, Springer, New York, 2013, pp. 285–318.

7. Wang, Q., Ping, P., Zhao, X., et al., "Thermal Runaway Caused Fire and Explosion of Lithium Ion Battery," *Journal of Power Sources*, Vol. 208, 2012, pp. 210–224.

8. Webster, H., "Flammability Assessment of Bulk-Packed, Rechargeable Lithium-Ion Cells in Transport Category Aircraft," FAA Report DOT/FAA/AR-06/38, September 2006.

9. Quintiere, J.G., Crowley, S.B., Walters, R.N., Lyon, R.E., and Blake, D., "Fire Hazards of Lithium Batteries," FAA Technical Note DOT/FAA/TC-TN15/17, June 2015.

10. Levine, I.A., *Physical Chemistry*, McGraw-Hill, Inc., New York, 1995, Chapter 5, Standard Thermodynamic Functions of Reaction, pp. 135–163.

11. "Standard Test Method for Gross Calorific Value of Coal and Coke," ASTM D 5865, American Society for Testing and Materials, West Conshohocken, Pennsylvania.

12. Walters, R.N. and Lyon, R.E., "Measuring Energy Release of Lithium Ion Battery Failure Using a Bomb Calorimeter," FAA Report DOT/FAA/TC-15/40, October 2015.

13. Lyon, R.E., "Thermal Dynamics of Bomb Calorimeters," *Review of Scientific Instruments*, Vol. 86, No. 125103, 2015.